

**The chiral phase transition for lattice QCD with 2 color-sextet quarks**

J. B. Kogut

*Department of Energy, Division of High Energy Physics, Washington, DC 20585, USA  
and Department of Physics, TQHN, University of Maryland, 82 Regents Drive,  
College Park, Maryland 20742, USA*

D. K. Sinclair

*HEP Division, Argonne National Laboratory, 9700 South Cass Avenue, Argonne, Illinois 60439, USA  
(Received 7 July 2015; published 21 September 2015)*

QCD with 2 flavors of massless color-sextet quarks is studied as a possible walking-Technicolor candidate. We simulate the lattice version of this model at finite temperatures near to the chiral-symmetry restoration transition, to determine whether it is indeed a walking theory (QCD-like with a running coupling which evolves slowly over an appreciable range of length scales) or if it has an infrared fixed point, making it a conformal field theory. The lattice spacing at this transition is decreased towards zero by increasing the number  $N_t$  of lattice sites in the temporal direction. Our simulations are performed at  $N_t = 4, 6, 8, 12$ , on lattices with spatial extent much larger than the temporal extent. A range of small fermion masses is chosen to make predictions for the chiral (zero mass) limit. We find that the bare lattice coupling does decrease as the lattice spacing is decreased. However, it decreases more slowly than would be predicted by asymptotic freedom. We discuss whether this means that the coupling is approaching a finite value as lattice  $N_t$  is increased—the conformal option, or if the apparent disagreement with the scaling predicted by asymptotic freedom is because the lattice coupling is a poor expansion parameter, and the theory walks. Currently, evidence favors QCD with 2 color-sextet quarks being a conformal field theory. Other potential sources of disagreement with the walking hypothesis are also discussed. We also report an estimate of the position of the deconfinement transition for  $N_t = 12$ , needed for choosing parameters for zero-temperature simulations.

DOI: [10.1103/PhysRevD.92.054508](https://doi.org/10.1103/PhysRevD.92.054508)

PACS numbers: 11.15.Ha, 12.60.Rc, 12.60.Fr, 12.38.Gc

**I. INTRODUCTION**

The LHC at CERN is currently probing the Higgs sector of the Standard Model of high-energy physics. This sector is the least well understood part of the Standard Model, and the least satisfactory from a theoretical standpoint. Thus the study of extensions of the Standard Model with a more aesthetically compelling Higgs sector is timely. The observation of a light ( $\approx 125$  GeV) Higgs-like excitation at ATLAS and CMS, with properties consistent with the Standard-Model Higgs, puts constraints on any such model. We are especially interested in those models where the Higgs sector is strongly coupled and the Higgs boson is composite.

We are interested in QCD-like models—non-Abelian gauge theories with massless fermions and spontaneously broken chiral symmetry—where the pionlike Goldstone bosons play the role of the Higgs field, giving mass to the  $W^\pm$  and  $Z$  weak vector bosons through the Higgs mechanism. Here the Higgs boson is the remnant radial excitation. Such theories are called Technicolor models [1,2]. Technicolor models, which are simply QCD scaled up so that  $f_\pi \approx 246$  GeV rather than  $f_\pi \approx 93$  MeV of regular QCD, are not phenomenologically viable. It has been suggested that Technicolor theories where the fermion content is such that the running gauge-coupling evolves

very slowly over an appreciable range of mass scales, described as “walking” rather than running, might be capable of overcoming such difficulties. Such theories are referred to as Walking Technicolor models [3–6]. Because of their nature, the nonperturbative properties of such models are amenable to study using the simulation methods developed for Lattice QCD. It is such theories that we are interested in simulating.

Candidate walking gauge theories typically have 2-loop  $\beta$ -functions with a second, nontrivial, zero. If this behavior remains true to all orders, this nontrivial fixed point controls the infrared properties of the theory, which is therefore a conformal field theory with a continuous spectrum. On the other hand, if the running coupling becomes so large that a chiral condensate forms before this would-be IR fixed point is reached, the theory is QCD-like with spontaneously broken chiral symmetry and Goldstone bosons separated by a mass gap from the rest of the spectrum. Because of the proximity of the would-be fixed point, a region where the coupling walks would be expected.

We have concentrated our efforts on techni-QCD with 2 flavors of massless Technicolor-sextet techniquarks. Since this is identical to QCD with 2 color-sextet quarks scaled so that  $f_\pi \approx 246$  GeV, we will omit the prefix “techni” from

here on. This theory has been identified as a potential walking-Technicolor candidate (see for example [7] and references therein). It is asymptotically free and its 2-loop  $\beta$ -function does have a nontrivial zero far enough from  $g^2 = 0$  for the coupling to become sufficiently large for there to be a chance that chiral symmetry breaks before it is reached. If it is indeed QCD-like, it has 3 Goldstone bosons, the correct number to give masses to the  $W$ s and  $Z$ , with none left over. In this sense, it is minimal.

Other groups have studied or are studying this model using lattice techniques. The main contributors are Degrand *et al.* [8–13] and the Lattice Higgs Collaboration [14–21], In addition we should mention some recent work by A. Hasenfratz and her collaborators [22]. With the exception of one early paper by Degrand *et al.* [9], these have concentrated on the zero-temperature properties of this model. We study lattice QCD with 2 color-sextet quarks at finite temperature. Our goal is to determine if the evolution of the coupling as lattice spacing  $a \rightarrow 0$  is described by asymptotic freedom, and that chiral symmetry remains broken in this limit. Assuming that the chiral-symmetry-restoration transition is indeed a finite-temperature transition, increasing the temporal extent of the lattice,  $N_t$  in lattice units, with the spatial extent  $N_s \gg N_t$ , and with temperature  $T$  fixed at the chiral phase transition temperature  $T_\chi$ , takes  $a = 1/N_t T_\chi$  towards zero. Thus the running coupling at this temperature,  $g_\chi(a)$ , should approach zero as  $N_t \rightarrow \infty$  in a manner determined by the perturbative  $\beta$ -function. If, on the other hand, the theory is conformal,  $g_\chi$  will approach a finite limit as  $N_t \rightarrow \infty$ , characterizing a bulk transition. Similar arguments should apply to the deconfinement transition at  $g_d$ . However, as we have determined, deconfinement occurs at a much stronger coupling than chiral-symmetry restoration. For the  $N_t$  values we have considered ( $N_t \leq 12$ ),  $g_d$  is too large for its evolution to be controlled by the perturbative  $\beta$ -function.

Recent use of this method, to search for the lower bound (in  $N_f$ ) of the conformal window for QCD with many fundamental quarks [23–26] have shown it to complement step-scaling methods. The reader should consult the references in these papers for the history of such studies. Although these methods are, in principle, straight forward, these recent papers indicate that they are not so easy to implement in practice.

Our earlier studies at  $N_t = 4, 6, 8$  [27,28] were consistent with the evolution of  $g_\chi$  between  $N_t = 6$  and  $N_t = 8$  being described by the 2-loop  $\beta$ -function. We have extended our simulations to  $N_t = 12$ . In addition, we have covered the neighborhood of the chiral transition for  $N_t = 6$  and  $N_t = 8$  with more closely spaced values of  $\beta = 6/g^2$  to determine  $g_\chi$  more precisely. In addition, we have determined the position of the deconfinement transition for  $N_t = 12$  for one mass value. Preliminary versions of the results presented in this paper have been presented at lattice conferences [29,30].

While the observed change in  $\beta_\chi = 6/g_\chi^2$  between  $N_t = 6$  and  $N_t = 8$  is consistent with that predicted using the 2-loop  $\beta$ -function, that between  $N_t = 8$  and  $N_t = 12$  is only about half the predicted value. At face value, this suggests that  $\beta_\chi$  could be approaching a finite limit, which would mean that this theory is conformal. However, we need to be cautious, since we are studying the evolution of the bare lattice coupling, which is known to be a poor choice of expansion parameters [31]. In addition, we are using unimproved staggered fermions for which perturbation expansions in terms of the bare lattice coupling are particularly poorly behaved, because of the “taste”-breaking tadpoles [32,33]. We discuss this and other potential sources of systematic errors in our approach, later in this paper. Our results make it important to perform further studies of lattice QCD with 3 massless, color-sextet quarks, to determine if it approaches its expected asymptotic behavior at  $N_t = 12$ , which would be qualitatively different from that observed for 2 flavors.

In Sec. II we discuss our methods of simulation and analysis. Section III gives the results of our simulations at  $N_t = 6, 8$  and 12 near the chiral transition. We compare these results with perturbative predictions in Sec. IV, and discuss improvements. In Sec. V we analyze simulations at  $N_t = 12$  in the neighborhood of the deconfinement transition. In Sec. VI we discuss our results, try to draw conclusions, and indicate directions for future studies.

## II. METHODS

This section largely repeats discussions given in earlier publications [27,28], and is included here for completeness. We use the simple Wilson plaquette action for the gauge fields:

$$S_g = \beta \sum_{\square} \left[ 1 - \frac{1}{3} \text{Re}(\text{Tr}UUUU) \right]. \quad (1)$$

Here the gauge fields  $U$  on the links are in the fundamental representation of  $SU(3)_{\text{color}}$ . We use the unimproved staggered-fermion action for the quarks:

$$S_f = \sum_{\text{sites}} \left[ \sum_{f=1}^{N_f/4} \psi_f^\dagger [\mathcal{D} + m] \psi_f \right], \quad (2)$$

where  $\mathcal{D} = \sum_{\mu} \eta_{\mu} D_{\mu}$  with

$$D_{\mu} \psi(x) = \frac{1}{2} [U_{\mu}^{(6)}(x) \psi(x + \hat{\mu}) - U_{\mu}^{(6)\dagger}(x - \hat{\mu}) \psi(x - \hat{\mu})], \quad (3)$$

where  $U^{(6)}$  is the sextet representation of  $U$ , i.e. the symmetric part of the tensor product  $U \otimes U$ . Reasons for this choice have been discussed in our earlier

publications. When  $N_f$  is not a multiple of 4 we use the fermion action:

$$S_f = \sum_{\text{sites}} \chi^\dagger \{[\mathcal{D} + m][-\mathcal{D} + m]\}^{N_f/8} \chi. \quad (4)$$

The operator which is raised to a fractional power is positive definite and we choose its positive-definite root. This yields a well-defined operator. We use the RHMC method for our simulations [34], where the required powers of the quadratic Dirac operator are replaced by diagonal rational approximations, to the desired precision. By applying a global Metropolis accept or reject step at the end of each trajectory, errors due to the discretization of molecular-dynamics “time” are removed.

The canonical partition function for a field theory at finite temperature  $T$  is realized by evaluating the functional integral for Euclidean time where the time is restricted to an interval  $1/T$  with periodic boundary conditions on the boson fields and antiperiodic boundary conditions on the fermion fields. Space is kept infinite. On a lattice of lattice spacing  $a$ , this means using a lattice of temporal extent  $N_t$  in lattice units where  $N_t a = 1/T$ . The spatial extent of the lattice  $N_s \gg N_t$ . For lattice QCD with sextet quarks, if deconfinement and chiral-symmetry restoration are finite-temperature transitions, then the associated temperatures at which they occur,  $T_d$  and  $T_\chi$  respectively, should be fixed, independent of  $a$ , for  $a$  small enough. Thus measuring the couplings at either of these transitions as  $N_t$  is varied, gives  $g(a)$  for a sequence of  $a$ s which approaches zero as  $N_t \rightarrow \infty$ . As it turns out  $\beta_d$  and hence  $g_d$  lies in the strong-coupling domain, outside the regime where perturbation theory is likely to be valid, for  $N_t = 4, 6, 8, 12$  and any other  $N_t$  which we are likely to consider in the near future. We therefore concentrate our efforts on the chiral transition, which occurs at much weaker couplings. If, on the other hand, QCD with 2 color-sextet quarks is conformal, the chiral transition would be a bulk transition. In this case  $g_\chi$  would approach a nonzero limit for large  $N_t$ , and the whole region of broken chiral symmetry would be a lattice artifact, disconnected from the conformal field theory at weaker coupling.

If QCD with 2 color-sextet quarks is QCD-like, the approach of  $g_\chi$  to zero is described by asymptotic freedom expressed in terms of the  $\beta$ -function. Through 2 loops this is given by:

$$\beta(g) = -b_1 g^3 - b_2 g^5. \quad (5)$$

Expressed in terms of  $\beta = 6/g^2$ , the evolution of the coupling when the lattice spacing is scaled by  $\lambda$  is given by

$$\begin{aligned} \Delta\beta(\beta) &= \beta(a) - \beta(\lambda a) \\ &= (12b_1 + 72b_2/\beta) \ln(\lambda) + \mathcal{O}(1/\beta^2), \end{aligned} \quad (6)$$

where for  $N_f$  flavors of color-sextet quarks:

$$\begin{aligned} b_1 &= \left(11 - \frac{10}{3}N_f\right)/16\pi^2 \\ b_2 &= \left(102 - \frac{250}{3}N_f\right)/(16\pi^2)^2. \end{aligned} \quad (7)$$

The chiral transition occurs at that value of  $\beta$  ( $\beta_\chi$ ) at which the chiral symmetry is restored and beyond which the chiral condensate  $\langle\bar{\psi}\psi\rangle$  vanishes, for massless quarks. Of course, in lattice simulations, we need to run at (small but) finite mass, and extrapolate to zero quark mass. It is not, however, practical to run at masses small enough for the condensate to accurately determine  $\beta_\chi$  directly. We therefore estimate  $\beta_\chi$  from the peaks in the chiral susceptibilities, or rather in the disconnected part of the chiral susceptibilities. This is given by:

$$\chi_{\bar{\psi}\psi} = V[\langle(\bar{\psi}\psi)^2\rangle - \langle\bar{\psi}\psi\rangle^2] \quad (8)$$

where the  $\langle\rangle$  indicates an average over the ensemble of gauge configurations and  $V$  is the space-time volume of the lattice. Since we use stochastic estimators for  $\bar{\psi}\psi$ , we need at least 2 estimators per configuration. The first term must include only contributions which are off diagonal in the noise, to obtain an unbiased estimator. We, in fact, use 5 stochastic estimators at the end of each trajectory giving 10 estimates for  $\chi_{\bar{\psi}\psi}$  per configuration.

### III. SIMULATIONS OF QCD WITH 2 FLAVORS OF COLOR-SEXTET QUARKS AT $N_f = 6, 8, 12$

Here we describe our simulations with 2 color-sextet quarks on lattices with  $N_f = 6, 8$  and 12. For  $N_f = 6$  and 8 we have extended the simulations of our earlier papers, where we simulated at  $\beta$  spacings of 0.1, through the chiral transition region. For the lowest mass ( $m = 0.005$ ) at  $N_f = 6$ , we have covered the vicinity of the chiral transition at  $\beta$  spacings of 0.02, and with increased statistics. At  $N_t = 8$  we have also covered the vicinity of the chiral transition with  $\beta$  spacings of 0.02 for all masses, including a new smaller mass ( $m = 0.0025$ ). We have performed new high-statistics simulations at  $N_t = 12$ , covering the region of the chiral transition with  $\beta$  spacings of 0.02, for all masses. Preliminary results of these new simulations have been presented at Lattice 2011, Lattice 2012, Lattice 2013 and Lattice 2014. In each case, we simulate using the RHMC algorithm with trajectory length 1. Most of our simulations have been performed on lattices with  $N_s = 2N_t$ .

#### A. $N_t = 6$

Our simulations at  $N_t = 6$  are performed on  $12^3 \times 6$  lattices with quark masses  $m = 0.005$ ,  $m = 0.01$  and

$m = 0.02$ . To more accurately pinpoint the peak of the chiral susceptibility at the lowest mass ( $m = 0.005$ ) we have covered the region in the neighborhood of the chiral transition  $6.5 \leq \beta \leq 6.7$  at  $\beta$  spacings of 0.02. At each of these  $\beta$ s we have performed runs of 100,000 trajectories. Outside of this interval, and that near the deconfinement regime, we employ  $\beta$  spacings of 0.1 and 10,000 trajectories per  $\beta$ . The chiral susceptibilities [Eq. (8)] from these new runs and those for  $m = 0.01$  from our earlier work are plotted in Fig. 1.

Here we attempted to determine the position of the peak of the  $m = 0.005$  susceptibility using Ferrenberg-Swendsen interpolation, but were unable to obtain consistent results. We therefore chose to fit the “data” with a smooth curve:

$$\chi_{\bar{\psi}\psi} = a - b(\beta - \beta_\chi)^2 - c(\beta - \beta_\chi)^3. \quad (9)$$

The rationale for this simple form is so that we can use the same form for each  $N_t$ . The second term is to give a simple parabolic fit to the peak. The third term is necessary because, as is obvious for the larger  $N_t$ s, the susceptibility is not symmetric around the peak. The value obtained for  $\beta_\chi$  from a fit using all  $\beta$ s in the range  $6.4 \leq \beta \leq 6.7$  is  $\beta_\chi = 6.611(3)$  for a fit with  $\chi^2/\text{DOF}$  (degree of freedom) = 1.55, which is acceptable. This fit is shown, superimposed on the data in Fig. 2.

### B. $N_t = 8$

We have extended our simulations at  $N_t = 8$  on a  $16^3 \times 8$  lattice. For the 3 masses considered in our earlier work,  $m = 0.005$ ,  $m = 0.01$  and  $m = 0.02$ , we have increased the

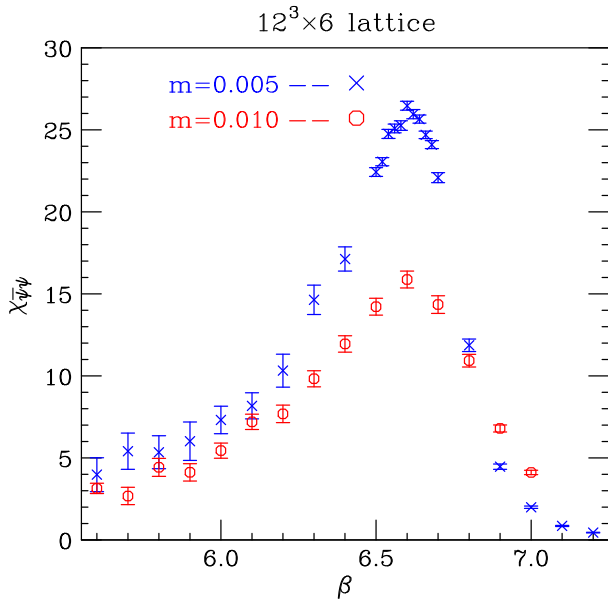


FIG. 1 (color online). Chiral susceptibilities on a  $12^3 \times 6$  lattice, with  $N_f = 2$ .

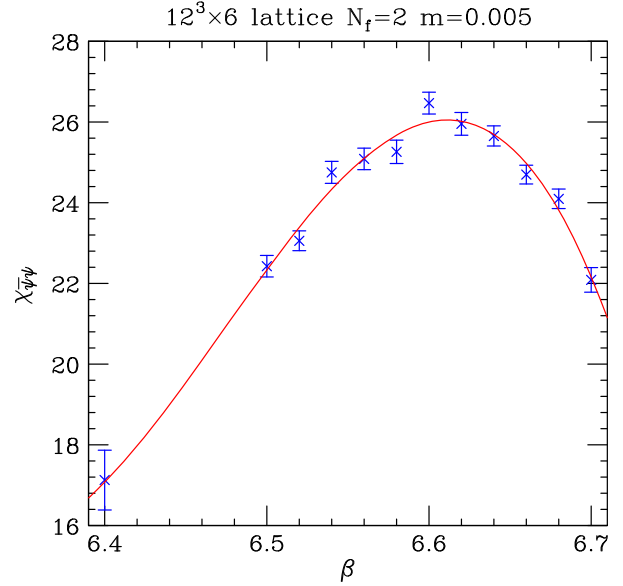


FIG. 2 (color online). Chiral susceptibilities on a  $12^3 \times 6$  lattice, with  $N_f = 2$   $m = 0.005$ . The curve is the fit described in the text, with  $a = 26.0489$ ,  $b = 407.578$ ,  $c = 978.166$  and  $\beta_\chi = 6.61143$ .

number of  $\beta$  values in the neighborhood of the chiral transition,  $6.6 \leq \beta \leq 6.8$ , by simulating at  $\beta$ s separated by 0.02 compared with our previous 0.1. We have increased our statistics to 50,000 trajectories at each  $(\beta, m)$  in this range. In addition, we have simulated at a new, lower mass,  $m = 0.0025$ . Again we have covered the range  $6.6 \leq \beta \leq 6.8$  with  $\beta$ s spaced by 0.02, performing runs of 100,000 trajectories at each  $\beta$ . Outside this range we performed a run of 20,000 trajectories at  $\beta = 6.5$ , and runs of 10,000 trajectories at  $\beta = 6.9$  and  $\beta = 7.0$ , for this smallest mass. Figure 3 shows the chiral susceptibilities for these runs.

To estimate the position of the peak of the chiral susceptibility for  $m = 0.0025$ , we first consider using Ferrenberg-Swendsen interpolation of the chiral susceptibilities. This is possible, since the distributions of plaquette values for adjacent  $\beta$ s in the range  $6.6 \leq \beta \leq 6.8$  show significant overlap. Here we performed extrapolations from the susceptibilities for  $\beta = 6.66$ ,  $\beta = 6.68$ ,  $\beta = 6.70$ ,  $\beta = 6.72$  and  $\beta = 6.74$ , and looked for consistency in our predictions. The best consistency we found was between extrapolations from  $\beta = 6.68$ , which predicted a peak at  $\beta = 6.691(24)$ , and  $\beta = 6.70$ , which predicted a peak at  $\beta = 6.689(5)$ . Combining these we obtain a prediction  $\beta_\chi = 6.69(1)$ .

A second estimate comes from fitting our susceptibilities to the form we used for  $N_t = 6$  [Eq. (9)]. For  $m = 0.0025$ , fitting to this cubic polynomial over all points in the range  $6.5 \leq \beta \leq 6.8$  yields  $\beta_\chi = 6.706(1)$  for the value of  $\beta$  at the peak. This fit has  $\chi^2/\text{DOF} = 0.55$ , which is excellent. Figure 4 shows this fit superimposed on the “data”. Performing a similar fit to the susceptibilities at



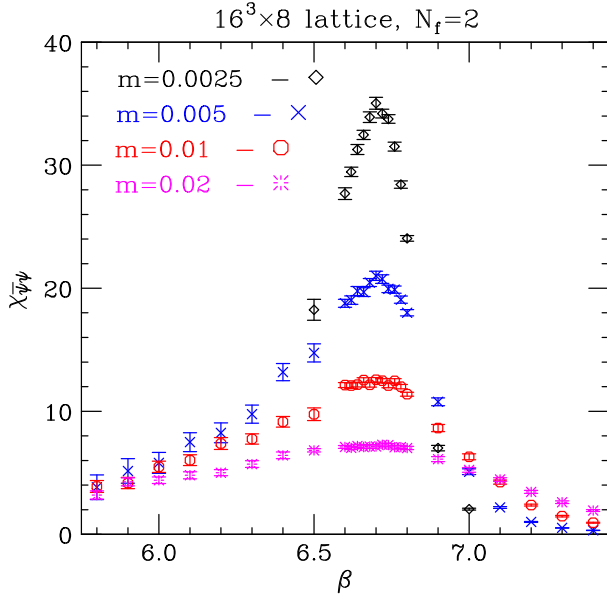


FIG. 3 (color online). Chiral susceptibilities on a  $16^3 \times 8$  lattice with  $N_f = 2$ .

$m = 0.005$  over the range  $6.5 \leq \beta \leq 6.9$  gives  $\beta_\chi = 6.701(4)$  with  $\chi^2/\text{DOF} = 0.85$ . Fitting the susceptibilities for  $m = 0.01$  over the range  $6.5 \leq \beta \leq 6.9$  yields  $\beta_\chi = 6.693(8)$  with  $\chi^2/\text{DOF} = 1.36$  while fits to the susceptibilities for  $m = 0.02$  over the same range predicts  $\beta_\chi = 6.71(1)$  with  $\chi^2/\text{DOF} = 0.29$ . A word of caution is due concerning the fits for the 2 largest masses. In both these cases, the measured susceptibility is statistically flat over an

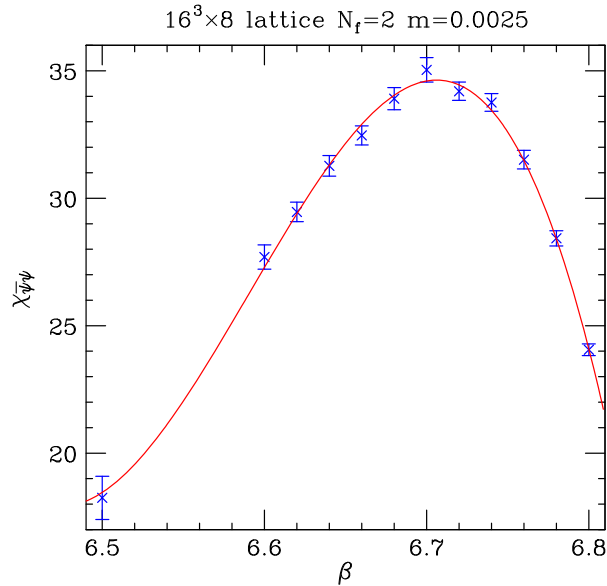


FIG. 4 (color online). Chiral susceptibilities on a  $16^3 \times 8$  lattice with  $N_f = 2$  and  $m = 0.0025$ . The curve is the fit described in the text, with  $a = 34.6359$ ,  $b = 940.687$ ,  $c = 2716.49$  and  $\beta_\chi = 6.70613$ .

appreciable neighborhood of the transition. The positions of these 2 peaks is thus determined largely by the outlying points on the fits, and should therefore not be taken too seriously. The main reason for performing these high-mass fits is to get an estimate of the height of these peaks from the parameter  $a$  in the fits.

For a second-order phase transition, the value  $\chi_{\bar{\psi}\psi}$  at the peak,  $\chi_{\text{max}}$  is expected to scale with mass as:

$$\chi_{\text{max}} = Am^{1/\delta-1}. \quad (10)$$

If the chiral transition is a finite-temperature transition, it is expected to lie in the  $O(2)$  or  $O(4)$  universality class where the critical exponent  $\delta \approx 4.8$ . If it is a bulk transition, which is expected to be first order,  $\delta = \infty$ . The best fit to Eq. (10) gives  $\delta = 4.1(1)$  and has  $\chi^2/\text{DOF} = 9$ . Figure 5 shows this fit superimposed on the values of  $\chi_{\text{max}}$  taken from the values of  $a$  in the susceptibility fits. Clearly the reason that the estimated quality of the fit (reduced  $\chi^2$ ) is poor is because the systematic errors associated with choosing  $a$  as an estimate for  $\chi_{\text{max}}$  have been ignored, whereas, especially for the larger masses, these clearly dominate.

At  $N_f = 8$ , we have also performed simulations with  $m = 0.0025$  on a  $24^3 \times 8$  lattice at 3  $\beta$  values, near and above the chiral transition, to check for finite volume effects. Values of the chiral susceptibilities, which should be most susceptible to finite volume effects, are given here, along with their values on a  $16^3 \times 8$  lattice in square brackets. For  $\beta = 6.7$ ,  $\chi_{\bar{\psi}\psi} = 34.4(4)[35.0(5)]$ , for  $\beta = 6.76$ ,  $\chi_{\bar{\psi}\psi} = 30.9(4)[31.5(4)]$ , while for  $\beta = 6.9$ ,  $\chi_{\bar{\psi}\psi} = 7.0(2)[7.0(2)]$ . These results are in good-enough agreement for us to conclude that finite volume effects are small at the masses we use.

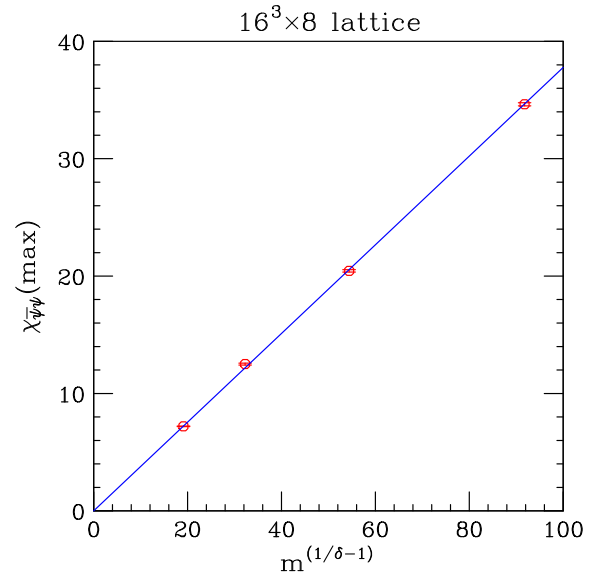


FIG. 5 (color online). Peak of chiral susceptibility as a function of mass, with fit to critical scaling form  $\chi_{\text{max}} = Am^{1/\delta-1}$  on a  $16^3 \times 8$  lattice.

**C.  $N_t = 12$**

We perform simulations on a  $24^3 \times 12$  lattice at masses  $m = 0.0025$ ,  $m = 0.005$  and  $m = 0.01$ , in the neighborhood of the chiral transition. At the smallest mass,  $m = 0.0025$ , we perform simulations at  $\beta$  values spaced by 0.02 over the range  $6.6 \leq \beta \leq 6.9$ . For  $6.6 \leq \beta \leq 6.66$  we perform runs of 50,000 trajectories at each  $\beta$ . For the range  $6.68 \leq \beta \leq 6.9$  we perform runs of 100,000 trajectories per  $\beta$ . At  $\beta = 6.5$ , we run for 25,000 trajectories, while for  $\beta = 7.0$ ,  $\beta = 7.1$  and  $\beta = 7.2$ , we perform runs of 10,000 trajectories per  $\beta$ . At mass  $m = 0.005$  we again cover the interval  $6.6 \leq \beta \leq 6.9$  at increments of 0.02. For  $\beta = 6.6$ , we run for 100,000 trajectories. For the rest of the interval i.e.  $6.62 \leq \beta \leq 6.9$  we run for 50,000 trajectories per  $\beta$ . At  $\beta = 6.5$  we run for 25,000 trajectories, while for  $\beta = 6.4$ ,  $\beta = 7.0$ ,  $\beta = 7.1$  and  $\beta = 7.2$ , we run for 10,000 trajectories per  $\beta$ . At  $m = 0.01$  we perform simulations of 25,000 trajectories per  $\beta$  at  $\beta$ s spaced by 0.02 over the range  $6.6 \leq \beta \leq 6.9$ . At  $\beta = 6.3, 6.4, 6.5$  we run for 25,000 trajectories per  $\beta$ , while for  $\beta = 6.2$  we run for 12,500 trajectories. For  $\beta = 6.0, 6.1$  and for  $\beta = 7.0, 7.1, 7.2$  we perform runs of 10,000 trajectories. We also run for 50,000 trajectories per  $\beta$  for  $\beta$ s spaced by 0.02 over the range  $5.7 \leq \beta \leq 5.9$ , which is in the neighborhood of the deconfinement transition. These runs at  $\beta < 6$  will be discussed further in Sec. V.

Figure 6(a) shows the chiral condensates ( $\langle \bar{\psi}\psi \rangle$ ), as functions of  $\beta$  for all 3 masses  $m = 0.0025$ ,  $m = 0.005$ ,  $m = 0.01$ . These are bare (lattice) quantities. However, at nonzero mass, if we expand in powers of the quark mass  $m$ , the coefficient of  $m$  in physical units diverges as  $1/a^2$  as  $a \rightarrow 0$ , and should be regularized. We therefore subtract part of this divergence using the prescription adopted by the Lattice Higgs Collaboration, where the subtracted chiral condensate is defined by:

$$\langle \bar{\psi}\psi \rangle_{\text{sub}} = \langle \bar{\psi}\psi \rangle - \left( m_V \frac{\partial}{\partial m_V} \langle \bar{\psi}\psi \rangle \right)_{m_V=m}, \quad (11)$$

where  $m_V$  is the valence-quark mass. What we observe is, that while the unsubtracted chiral condensate shows indications that it will vanish in the chiral ( $m \rightarrow 0$ ) limit for  $\beta$  sufficiently large, the subtracted chiral condensate shows this vanishing more clearly. However, even the subtracted chiral condensate does not yield an estimate for  $\beta_\chi$  which is accurate enough for our purposes. We thus turn to using the peaks of the chiral susceptibilities, extrapolated to zero mass as our estimates for  $\beta_\chi$ .

Figure 7 shows the chiral susceptibilities, defined in Eq. (8) extracted from our measurements of  $\langle \bar{\psi}\psi \rangle$  (5 per trajectory) in our simulations on  $24^3 \times 12$  lattices for masses  $m = 0.0025$ ,  $m = 0.005$  and  $m = 0.01$ . Here, the distributions of plaquette values for adjacent  $\beta$ s have insufficient overlap to even attempt using Ferrenberg-Swendsen interpolation to estimate the positions of the

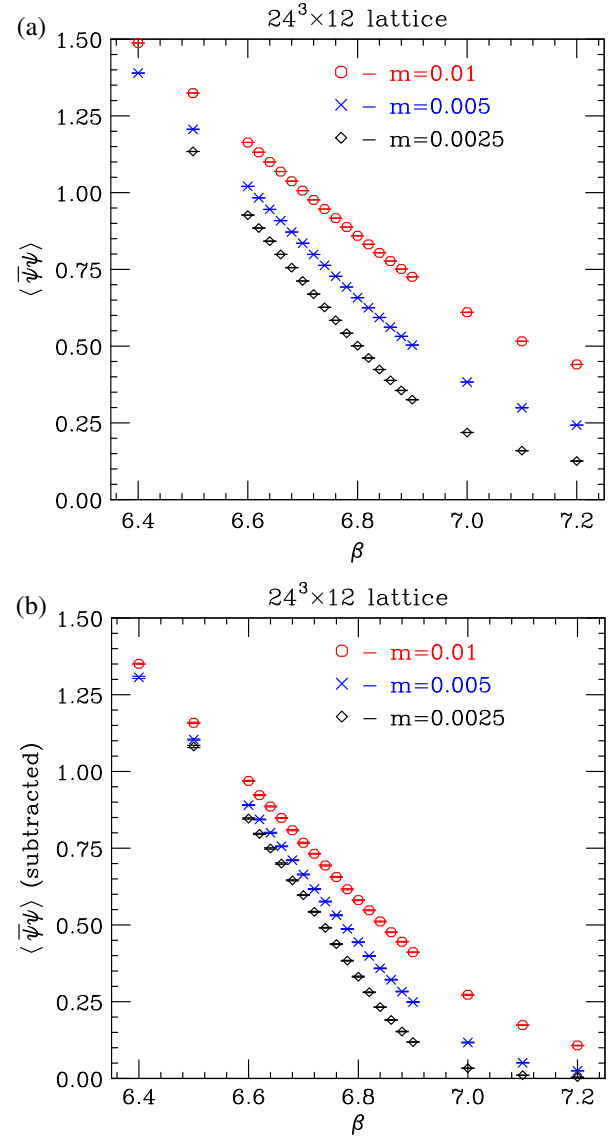


FIG. 6 (color online). (a) Unsubtracted chiral condensates  $\langle \bar{\psi}\psi \rangle$  as functions of  $\beta$  for masses  $m = 0.0025, 0.005, 0.01$ . (b) Chiral condensates  $\langle \bar{\psi}\psi \rangle$ , subtracted using the Lattice Higgs Collaboration’s prescription, as functions of  $\beta$  for masses  $m = 0.0025, 0.005, 0.01$ .

peaks in the susceptibilities for the 3 masses. The susceptibilities for  $m = 0.0025$  show a clear peak, those for  $m = 0.005$  show some indication of a rather flat peak, while those for  $m = 0.01$  show little evidence for any peak. In order to extract an estimate of the positions of these peaks, we use the fitting form used for  $N_t = 6$  and 8 [Eq. (9)], which makes maximal use of the “data”. The fit to the  $m = 0.0025$  susceptibilities for all points in the range  $6.5 \leq \beta \leq 6.9$  yields  $\beta_\chi = 6.768(2)$  in an acceptable fit with  $\chi^2/\text{DOF} = 1.68$ . This fit is superimposed over the measured susceptibilities in Fig. 8. A fit to the  $m = 0.005$  “data” over the same interval predicts  $\beta_\chi = 6.745(6)$  with  $\chi^2/\text{DOF} = 0.91$ , while a fit to the  $m = 0.01$  data also over

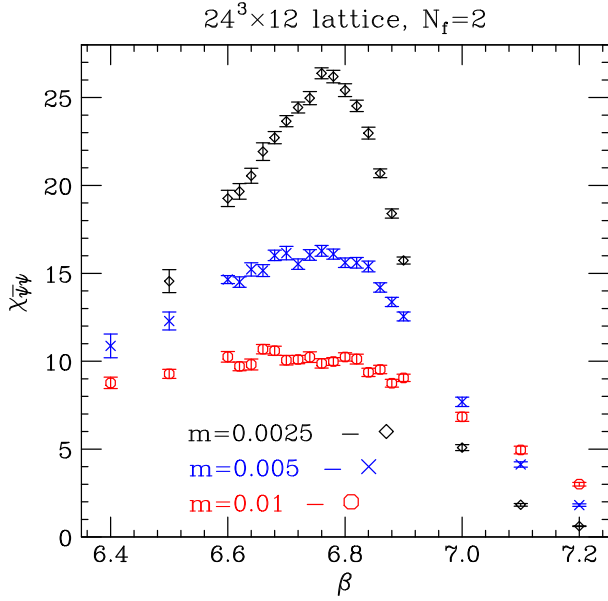


FIG. 7 (color online). Chiral susceptibilities on a  $24^3 \times 12$  lattice with  $N_f = 2$ .

the same range gives  $\beta_\chi = 6.70(3)$  with  $\chi^2/\text{DOF} = 1.52$ . These last 2 fits should not be considered too seriously, because these peaks are defined by outlying rather than central points, owing to the flatness of the distributions. Their main purpose is to yield an estimate for the values of the parameter  $a$  at their peaks.

We also consider the scaling properties of the susceptibility peak with mass using the scaling form of Eq. (10). With only 3 points, there is only one degree of freedom.

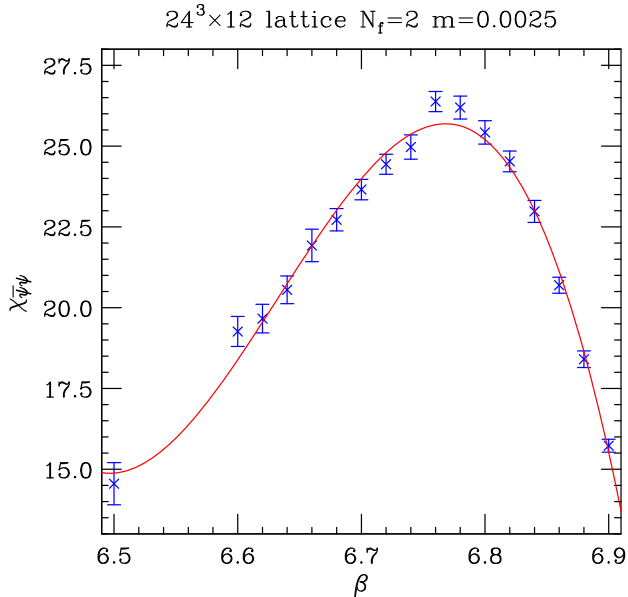


FIG. 8 (color online). Chiral susceptibilities on a  $24^3 \times 12$  lattice with  $N_f = 2$  and  $m = 0.0025$ . The curve is the fit described in the text, with  $a = 25.691$ ,  $b = 440.589$ ,  $c = 1082.3$  and  $\beta_\chi = 6.76801$ .

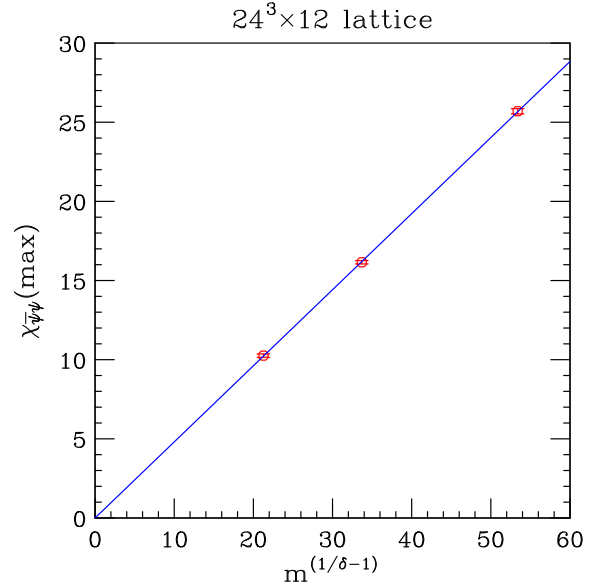


FIG. 9 (color online). Peak of chiral susceptibility as a function of mass, with fit to critical scaling form  $\chi_{\max} = Am^{1/\delta-1}$  on a  $24^3 \times 12$  lattice.

Our fit gives the critical exponent  $\delta = 2.98(4)$  with  $\chi^2/\text{DOF} = 0.29$ . This is in agreement with the mean-field (free-field) critical exponent  $\delta = 3$ , rather than the expected  $O(2)$  or  $O(4)$  critical exponent  $\delta \approx 4.8$  or first-order scaling  $\delta = \infty$ . The graph of our data—the values of  $a$  from our fits—with this fit superimposed is given in Fig. 9.

#### IV. COMPARISON WITH PERTURBATIVE PREDICTIONS

Here for consistency we only consider the values of  $\beta_\chi$  obtained from fitting our chiral susceptibilities to the form given in Eq. (9). The errors given in the previous section do not include any systematic errors due to this rather arbitrary choice of a fitting function or to the selection of the range of  $\beta$  values over which the fits are performed. We will assume 0.01 as a conservative estimate of these systematic errors, at least for the lightest masses. Because our measurements are inadequate to reliably determine if there is any significant mass dependence on the position of the peaks, we take our measurement of the position of the peak for the lightest mass as our estimate for the position of the transition in the chiral limit. We assume that our estimate of the systematic errors is large enough to encompass the shift in the positions of the peaks as we approach the chiral limit. Table I summarizes the results of our determinations of the positions of the chiral transitions ( $\beta_\chi$ ) from this and previous publications, as well as those of the positions of the deconfinement transitions ( $\beta_d$ ) from previous publications and the next section.

Equation (6) gives the perturbative asymptotic freedom predictions for the changes in  $\beta_\chi$  between different  $N_f$ s. In particular:

TABLE I.  $N_f = 2$  deconfinement and chiral transitions for  $N_t = 4, 6, 8, 12$ .

$N_t$	$\beta_d$	$\beta_\chi$
4	5.40(1)	6.3(1)
6	5.54(1)	6.61(1)
8	5.65(1)	6.71(1)
12	5.81(1)	6.77(1)

$$\begin{aligned}
 \beta_\chi(N_t = 8) - \beta_\chi(N_t = 6) &\approx 0.087 \\
 \beta_\chi(N_t = 12) - \beta_\chi(N_t = 8) &\approx 0.122 \\
 \beta_\chi(N_t = 12) - \beta_\chi(N_t = 6) &\approx 0.209. \tag{12}
 \end{aligned}$$

The reason for including the third equation is because, if this is a finite temperature transition, the fermion mass in physical units for  $m = 0.005$  at  $N_t = 6$  and for  $m = 0.0025$  at  $N_t = 12$  are identical, so that one might hope that any error due to not extrapolating to the chiral limit might be minimized. Our measurements (from Table I) give

$$\begin{aligned}
 \beta_\chi(N_t = 8) - \beta_\chi(N_t = 6) &= 0.10(1) \\
 \beta_\chi(N_t = 12) - \beta_\chi(N_t = 8) &= 0.06(1) \\
 \beta_\chi(N_t = 12) - \beta_\chi(N_t = 6) &= 0.16(1). \tag{13}
 \end{aligned}$$

If taken at face value, these favor the conformal option, where the fact that  $\beta_\chi(N_t = 12) - \beta_\chi(N_t = 8)$  is roughly half the value predicted by asymptotic freedom could indicate that  $\beta_\chi$  is approaching a nonzero limit.

We need to be cautious, since the lattice coupling and hence  $1/\beta$  is known to be a poor expansion parameter. That is, higher order terms for the expansion of any quantity in powers of  $g^2$  tend to be large. The simplest improved choice of  $\beta$ s is the tadpole-improved  $\beta$  of Lepage and Mackenzie [31]:

$$\bar{\beta} = \frac{1}{3} \langle \text{Tr}_\square UUUU \rangle \beta. \tag{14}$$

For connection with Lepage-Mackenzie,  $\bar{\beta} = 6/\bar{g}^2 = 6/4\pi\bar{\alpha}$ . (Note that for staggered fermions, tadpole improvement of the fermion determinant is equivalent to rescaling the fermion mass and can thus be ignored, since we are interested in the limit  $m \rightarrow 0$ .) The plaquette in the above equation should be evaluated at  $\beta$ , on a lattice which is at zero temperature. Since  $T = 0$ , in practice means on an  $N_t^4$  lattice for which  $\beta \ll \beta_d(N_t)$ , this would require simulating on lattices much larger than any we contemplate. For this reason, we use the finite temperature plaquettes from our simulations in this equation. This yields  $\bar{\beta}_\chi(N_t = 6) = 4.48(1)$ ,  $\bar{\beta}_\chi(N_t = 8) = 4.58(1)$  and  $\bar{\beta}_\chi(N_t = 12) = 4.65(1)$ . This gives

$$\begin{aligned}
 \bar{\beta}_\chi(N_t = 8) - \bar{\beta}_\chi(N_t = 6) &= 0.10(1) \\
 \bar{\beta}_\chi(N_t = 12) - \bar{\beta}_\chi(N_t = 8) &= 0.07(1) \\
 \bar{\beta}_\chi(N_t = 12) - \bar{\beta}_\chi(N_t = 6) &= 0.17(1). \tag{15}
 \end{aligned}$$

compared with the perturbative prediction:

$$\begin{aligned}
 \bar{\beta}_\chi(N_t = 8) - \bar{\beta}_\chi(N_t = 6) &\approx 0.083 \\
 \bar{\beta}_\chi(N_t = 12) - \bar{\beta}_\chi(N_t = 8) &\approx 0.117 \\
 \bar{\beta}_\chi(N_t = 12) - \bar{\beta}_\chi(N_t = 6) &\approx 0.200. \tag{16}
 \end{aligned}$$

While this is an overall improvement, it is insufficient. Choosing instead  $\beta_V$ , the  $\beta$  associated with the interquark potential, makes little difference. Here  $\beta_V = 6/g_V^2 = 6/4\pi\alpha_V$ . We use the relation between  $\bar{\alpha}$  and  $\alpha_V$  from Lepage-Mackenzie to obtain  $\beta_V$ . The reason that going from  $\beta$  to  $\beta_V$  does not make much difference is because, as noted by Lepage-Mackenzie, the perturbative relation:

$$\beta = \beta_V + 2.245 + \mathcal{O}(1/\beta_V) \tag{17}$$

(where we have chosen the momentum scale at which we measure  $\beta_V$  to be  $\pi/a$ ), is a good approximation. With such a constant shift, differences in  $\beta$ s are left unchanged. In the prediction, based on the perturbative  $\beta$ -function, for the  $\beta$ s ( $\beta_V$ s) we consider, the 2-loop contribution is small, so the perturbative predictions for differences in  $\beta$ s and  $\beta_V$ s are almost the same. Here we see that replacing the lattice coupling with an improved coupling such as  $g_V$  does not significantly affect changes in  $\beta$ , since  $g$  is small enough that the 2-loop contribution to the  $\beta$ -function is significantly smaller than the 1-loop contribution, for both the original and improved schemes. Remember that the 1- and 2-loop coefficients in the  $\beta$ -function are scheme independent. Hence changing from lattice to improved couplings will not significantly improve agreement between measured and predicted running of the couplings. Of course, choosing a *much* smaller momentum scale for  $\beta_V$ , driving it towards the perturbative fixed point, could improve agreement for  $\beta_\chi(N_t = 12) - \beta_\chi(N_t = 8)$ , but would be difficult to justify.

However, it is well-known that even with tadpole improvement of the gauge links, perturbation theory for staggered fermions is still badly behaved [32,33]. The reason is another form of tadpole, the ‘‘doubler tadpole’’ due to flavor(‘‘taste’’)-mixing responsible for taste breaking. Unfortunately for us, before an improved perturbation theory could be developed for staggered fermions, interest shifted to improved staggered fermions designed to minimize taste breaking, making perturbation theory better behaved.

It is interesting to note that the lack of significant improvement using  $\bar{\beta}$  (or  $\beta_V$  or  $\beta_{\overline{\text{MS}}}$ ) instead of  $\beta$  has also been noticed by [23] in their studies of QCD with 8



TABLE II. Difference between the changes in the lattice  $\beta_c$  with change in  $N_t$  and the prediction from the 2-loop perturbative  $\beta$ -function, compared with the same quantity using the improved  $\beta_c$ , for quenched lattice QCD.

$N_t$	$N_t'$	$1 - \frac{ \beta_c(N_t') - \beta_c(N_t) _{\text{lattice}}}{ \beta_c(N_t') - \beta_c(N_t) _{2\text{-loop}}}$	$1 - \frac{ \tilde{\beta}_c(N_t') - \tilde{\beta}_c(N_t) _{\text{lattice}}}{ \tilde{\beta}_c(N_t') - \tilde{\beta}_c(N_t) _{2\text{-loop}}}$
6	8	34%	19%
8	12	24%	13%
12	18	17%	8%

fundamental quarks using an improved staggered-quark action, so perhaps it is a property of theories with slowly varying running couplings and not an artifact of using unimproved actions. This contrasts with the one system where there are precise measurements of the finite temperature transition for a large range of  $N_t$  values, namely pure  $SU(3)$  Yang-Mills theory (quenched QCD) transcribed to the lattice using the Wilson (plaquette) action. For this system using an improved coupling greatly improves the agreement between the measured  $N_t$  dependence of the critical coupling  $\beta_c$  and the prediction from the 2-loop  $\beta$ -function, as shown in Table II. For these calculations we used the values of  $\beta_c(N_t)$  for quenched lattice QCD given in the recent publication [35].

## V. THE $N_t = 12$ DECONFINEMENT TRANSITION

In Sec. III we mentioned that we have extended our simulations on a  $24^3 \times 12$  lattice at  $m = 0.01$  into the neighborhood of the deconfinement transition. Although  $\beta_d$  is too small for its evolution to be governed by perturbation

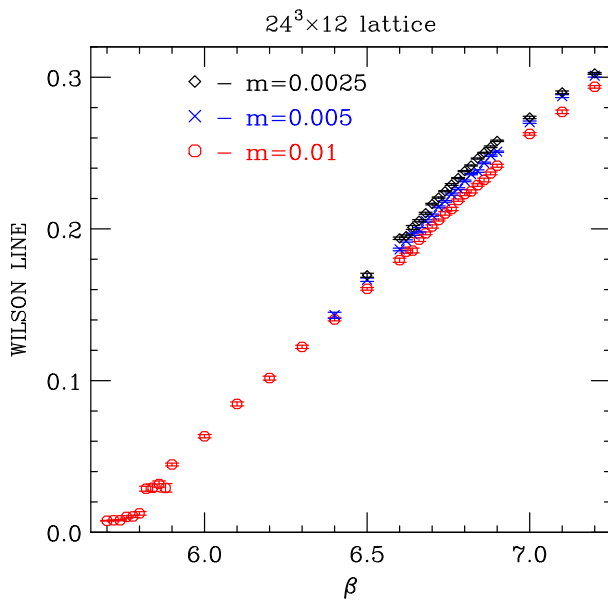


FIG. 10 (color online). Wilson Lines as functions of  $\beta$  on a  $24^3 \times 12$  lattice. These are traces of products gauge links in the color-triplet representation of  $SU(3)_{\text{color}}$ .

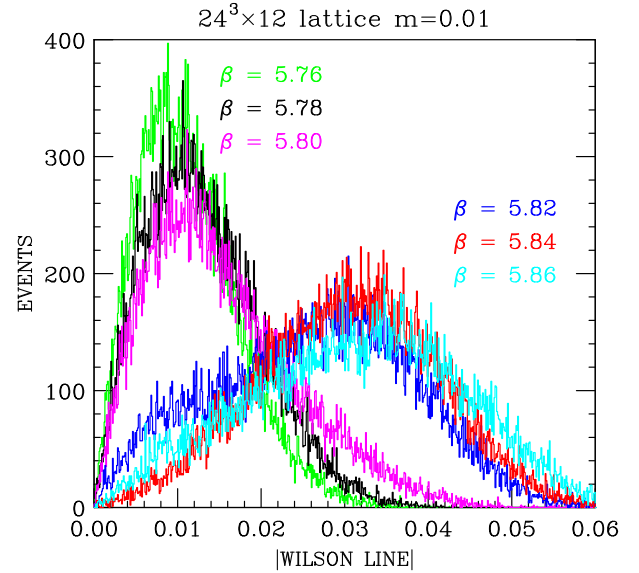


FIG. 11 (color online). Histograms of magnitudes of the Wilson Line for  $\beta$  values close to the deconfinement transition on a  $24^3 \times 12$  lattice with  $m = 0.01$ .

theory, knowledge of its value as a function of  $N_t$  is necessary when choosing  $\beta$  values for zero temperature simulations. It is also useful to know the value of the deconfinement temperature as well as the chiral-symmetry restoration temperature in physical units i.e. in terms of  $f_\pi \approx 246$  GeV. We chose to simulate this regime at only one quark mass so that we could devote most of our resources to the proximity of the chiral transition. For this same reason we chose the highest of our 3 masses. Here we are relying on the observation based on our studies at smaller  $N_t$ s that  $\beta_d$  depends only weakly on the quark mass.

The position of the deconfinement transition is determined by the point below which the Wilson Line (Polyakov Loop) becomes very small. Figure 10 is a plot of Wilson Lines against  $\beta$  for our  $24^3 \times 12$  simulations at all 3 masses. For the  $m = 0.01$  plot, we notice that the Wilson Line is near zero for small  $\beta$ s and then jumps to a value appreciably greater than zero at  $\beta \approx 5.8$ .

To determine the position of this deconfinement transition more precisely, we ran for 50,000 trajectories per  $\beta$  for  $\beta$  values spaced by 0.02 over the interval  $5.7 \leq \beta \leq 5.9$ . Figure 11 shows histograms of the distribution of magnitudes of the Wilson Line, for  $\beta$  values close to the deconfinement transition. Note the qualitative difference between these histograms for  $\beta \leq 5.80$  and those for  $\beta \geq 5.82$ . Those histograms for the lower range of  $\beta$ s are peaked at  $\approx 0.01$ , while those for  $\beta$ s in the upper range are peaked at  $\approx 0.03$ . From this we estimate that the deconfinement transition occurs at  $\beta = \beta_d = 5.81(1)$ . The transition is very abrupt, suggestive of a first-order phase transition. This value for  $\beta_d$  has been entered in Table I in Sec. IV.

## VI. DISCUSSION AND CONCLUSIONS

We use studies of scaling of the assumed finite-temperature chiral transition of lattice QCD with 2 color-sextet quarks to attempt to determine whether this theory is conformal or walking. This provides an alternative to the use of step-scaling methods to achieve this goal. Recent extensive step-scaling studies using improved staggered quarks [21] indicate that this theory walks, while similar studies using improved Wilson quarks [22] present evidence for a fixed point, which would mean that the theory is conformal. Hence use of a different method to try and determine which is the correct behavior is warranted.

We simulate lattice QCD with 2 flavors of color-sextet quarks on lattices with  $N_t = 6, 8$  and 12 in the vicinity of the chiral-symmetry restoration transition, to accurately determine the value  $\beta_\chi$  of  $\beta = 6/g^2$  at that transition. Under the assumption that this is a finite-temperature phase transition, which thus occurs at a fixed temperature in physical units, this gives the running of the gauge coupling  $g$  as the lattice spacing  $a$  is decreased. We compare the evolution of the coupling  $g_\chi$  at this transition with the prediction from the 2-loop perturbative  $\beta$ -function. What we find is that the change in  $\beta_\chi = 6/g_\chi^2$  is in approximate agreement with the perturbative prediction between  $N_t = 6$  and 8, but is smaller by about a factor of 2 than the prediction between  $N_t = 8$  and 12. This suggests that this chiral transition is a bulk transition for which  $\beta_\chi$  would approach a finite value in the large  $N_t$  limit. In this case this theory would be a conformal field theory, and not the desired walking theory. On the other hand, the scaling of the susceptibility peaks with mass suggests that the chiral transition is second order, whereas the simplest scenario for a bulk transition suggests that it should be first order. However, the fact that the critical exponent  $\delta \approx 3$  suggests that the transition is mean-field, which would be more likely for a true 4-dimensional and hence bulk transition, than for a finite-temperature and hence quasi-3-dimensional transition, which should be in the universality class of the 3-dimensional  $O(2)$  or  $O(4)$  spin model with  $\delta \approx 4.8$ .

In our initial comparison, we used the prediction in terms of the bare lattice coupling  $g(a)$ , which is known to be a poor expansion parameter. We therefore looked at the tadpole-improved coupling  $\bar{g}$ , which is supposed to be a better expansion parameter, as well as the related coupling  $g_V$  which is related to the heavy-quark potential. Both these improvements make a slight improvement in the running of the coupling, but not nearly enough to produce agreement with the perturbative results. (Based on our experience with quenched QCD we would have expected an agreement to within 20% or probably better.) We do note, however, that even when such improvements are applied, perturbation theory with unimproved staggered quarks does not work well. In addition, the examples where use of such couplings

( $\bar{g}$ ,  $g_V$  or  $g_{\overline{\text{MS}}}$ ) has improved the behavior of lattice perturbation theory have been for theories such as QCD with quarks in the fundamental representation of the color group, where the massless theory has only one mass or length scale, the scale associated with confinement and chiral symmetry breaking. For QCD with color-sextet quarks, we have shown that the scales of confinement and chiral-symmetry breaking are very different. It is unclear if methods which work for a single-scale theory will continue to work for a two-scale theory.

We note that use of staggered quarks and, in particular, unimproved staggered quarks, has potential difficulties because flavor symmetry (sometimes referred to as taste symmetry) is explicitly broken, and is only restored in the continuum limit. This means that in the chiral limit at nonzero lattice spacing, there are less massless degrees of freedom than in the continuum limit. Because of this, it is possible that a theory with an infrared fixed point and hence conformal, could appear to be walking. Hence, care needs to be taken in taking the continuum and chiral limits. Using an improved action can reduce these problems. However, improved staggered fermions have their own difficulties. Improving the staggered-fermion action can introduce extra phases which are lattice artifacts. This was observed in studies of the apparent bulk transition in QCD with 12 fundamental quarks [36,37] and provides extra complications for studying the finite temperature behavior of QCD with many fundamental quarks [23–26]. Improvement is designed to produce actions whose weak coupling physics is closer to that of the continuum theory. However, it does not necessarily produce better behavior in the intermediate or strong-coupling domain.

Another word of caution is necessary concerning our results. We have only used one spatial size ( $24^3$ ) for our  $N_t = 12$  simulations, so we have not ruled out finite volume effects. The mass dependence of the position of the peaks in chiral susceptibilities has not been adequately explored to check that we are really seeing the chiral limit. We have only used one action, and have not explored whether improved actions such as those used by the Lattice Higgs Collaboration and Degrand *et al.* might show different behavior.

While the most direct way of answering these questions would be to continue our work to lattices with larger  $N_t$  values and smaller quark masses, such simulations would be expensive, and it is not clear if repeating our studies with  $N_t = 16$  or 18 would provide the desired clarification. There are, however, other less expensive studies which could potentially help clarify the situation. The first, which we are pursuing, is to extend our simulations of QCD with 3 color-sextet quarks to  $N_t = 12$ . This theory is almost certainly conformal, and even if it is not, the perturbative evolution of its coupling is extremely slow (this is because asymptotic freedom is lost at  $N_f = 3 \frac{3}{10}$  for QCD with  $N_f$  sextet-quark flavors). Hence we should expect to see

essentially no change in the value of  $\beta_\chi$  between  $N_t = 8$  and  $N_t = 12$ . If this is observed it would indicate that the  $N_f = 2$  and  $N_f = 3$  theories are behaving rather differently as would be expected if the  $N_f = 2$  theory walks.

One method of testing how well some of the different choices of improved couplings work with sextet quarks and its 2 length scales would be to perform an extensive study of the position of the chiral transition with sextet quarks in the quenched theory. That this transition is separated from the deconfinement transition was shown in very early studies [38]. The advantage of this approach is that the production of very large quenched lattices can be performed very cheaply, and multimass inversions, already used in the RHMC algorithm will allow us to study the chiral condensate over a large range of masses. Here it will be possible compare the evolution of  $\beta_d$  and  $\beta_\chi$  with various improved couplings.

Another direction we are pursuing<sup>1</sup> is to simulate QCD with 2 color-sextet quarks at a fixed  $\beta$  value above  $\beta_\chi(N_t = 12)$ —we choose  $\beta = 6.9$ —and simulate on lattices with a fixed spatial volume, varying  $N_t$  to look for the transition. Perturbation theory predicts that  $\beta_\chi = 6.9$  for some  $N_t$  in the range  $18 < N_t < 20$ . We are simulating on  $24^3 \times N_t$  lattices with  $8 \leq N_t \leq 24$  with masses as low as  $m = 0.00125$ . Indications are that we will need to increase the spatial box size to accommodate the larger  $N_t$  s, since we are seeing finite volume effects at  $N_t = 22$  and 24.

<sup>1</sup>We thank Julius Kuti for this suggestion.

Temporarily ignoring questions as to whether this theory is QCD-like, we have started zero-temperature simulations at  $\beta = 5.81$  ( $\beta_d$  for  $N_t = 12$ ), on  $24^3 \times 48$  lattices. One of the reasons for this parameter choice, is to answer another question posed by Julius Kuti, who asked what value we estimate for  $T_d/f_\pi$ . So far we have produced 250 lattices separated by 100 trajectories for  $m = 0.01$  ( $m_\pi \approx 0.25$ ) and 250 lattices for  $m = 0.005$  ( $m_\pi \approx 0.175$ ). Larger-lattice zero-temperature simulations at weaker couplings are being contemplated.

Note that all the simulations reported in this paper are in the state where the argument of the Wilson Line (Polyakov Loop) is close to zero. Those states where the argument of the Wilson Line is close to  $\pm 2\pi/3$  are being ignored, except for  $\beta$ s approaching  $\beta_d$  and below, where transitions between these 3 states are frequent. However, should these be the true vacua, charge conjugation would be spontaneously broken [9], and so presumably would  $CP$ . If so, this could possibly provide a mechanism for baryogenesis.

## ACKNOWLEDGMENTS

DKS is supported in part by US Department of Energy Contract No. DE-AC02-06CH11357. These simulations were performed on Hopper, Edison, and Carver at NERSC, and Kraken at NICS and Stampede at TACC under XSEDE Project No. TG-MCA99S015, and Fusion and Blues at LCRC, Argonne. NERSC is supported by DOE Contract No. DE-AC02-05CH11231. XSEDE is supported by NSF Grant No. ACI-1053575. We thank members of the Lattice Higgs Collaboration for informative discussions.

- 
- [1] S. Weinberg, *Phys. Rev. D* **19**, 1277 (1979).
  - [2] L. Susskind, *Phys. Rev. D* **20**, 2619 (1979).
  - [3] B. Holdom, *Phys. Rev. D* **24**, 1441 (1981).
  - [4] K. Yamawaki, M. Bando, and K. i. Matumoto, *Phys. Rev. Lett.* **56**, 1335 (1986).
  - [5] T. Akiba and T. Yanagida, *Phys. Lett.* **169B**, 432 (1986).
  - [6] T. W. Appelquist, D. Karabali, and L. C. R. Wijewardhana, *Phys. Rev. Lett.* **57**, 957 (1986).
  - [7] D. D. Dietrich and F. Sannino, *Phys. Rev. D* **75**, 085018 (2007).
  - [8] Y. Shamir, B. Svetitsky, and T. DeGrand, *Phys. Rev. D* **78**, 031502 (2008).
  - [9] T. DeGrand, Y. Shamir, and B. Svetitsky, *Phys. Rev. D* **79**, 034501 (2009).
  - [10] T. DeGrand, *Phys. Rev. D* **80**, 114507 (2009).
  - [11] T. DeGrand, Y. Shamir, and B. Svetitsky, *Phys. Rev. D* **82**, 054503 (2010).
  - [12] T. DeGrand, Y. Shamir, and B. Svetitsky, *Phys. Rev. D* **87**, 074507 (2013).
  - [13] T. DeGrand, Y. Shamir, and B. Svetitsky, *Phys. Rev. D* **88**, 054505 (2013).
  - [14] Z. Fodor, K. Holland, J. Kuti, D. Negradi, and C. Schroeder, *J. High Energy Phys.* **11** (2009) 103.
  - [15] Z. Fodor, K. Holland, J. Kuti, D. Negradi, and C. Schroeder, *Proc. Sci.*, LATTICE2010 (2010) 060, [arXiv:1103.5998](#).
  - [16] Z. Fodor, K. Holland, J. Kuti, D. Negradi, C. Schroeder, and C. H. Wong, *Phys. Lett. B* **718**, 657 (2012).
  - [17] Z. Fodor, K. Holland, J. Kuti, D. Negradi, C. Schroeder, and C. H. Wong, *Proc. Sci.*, LATTICE2012 (2012) 025.
  - [18] Z. Fodor, K. Holland, J. Kuti, D. Negradi, and C. H. Wong, *Proc. Sci.*, LATTICE2013 (2014) 062.
  - [19] Z. Fodor, K. Holland, J. Kuti, S. Mondal, D. Negradi, and C. H. Wong, *Proc. Sci.*, LATTICE2014 (2015) 244.
  - [20] Z. Fodor, K. Holland, J. Kuti, S. Mondal, D. Negradi, and C. H. Wong, *Proc. Sci.*, LATTICE2014 (2015) 270.
  - [21] Z. Fodor, K. Holland, J. Kuti, S. Mondal, D. Negradi, and C. H. Wong, [arXiv:1506.06599](#).

- [22] A. Hasenfratz, Y. Liu, and C. Y. H. Huang, [arXiv:1507.08260](#).
- [23] A. Deuzeman, M. P. Lombardo, and E. Pallante, *Phys. Lett. B* **670**, 41 (2008).
- [24] A. Deuzeman, M. P. Lombardo, and E. Pallante, *Phys. Rev. D* **82**, 074503 (2010).
- [25] D. Schaich, A. Cheng, A. Hasenfratz, and G. Petropoulos, *Proc. Sci.*, LATTICE2012 (2012) 028.
- [26] D. Schaich *et al.* (LSD Collaboration), [arXiv:1506.08791](#).
- [27] J. B. Kogut and D. K. Sinclair, *Phys. Rev. D* **81**, 114507 (2010).
- [28] J. B. Kogut and D. K. Sinclair, *Phys. Rev. D* **84**, 074504 (2011).
- [29] D. K. Sinclair and J. B. Kogut, *Proc. Sci.*, LATTICE2012 (2012) 026.
- [30] D. K. Sinclair and J. B. Kogut, *Proc. Sci.*, LATTICE2014 (2014) 239.
- [31] G. P. Lepage and P. B. Mackenzie, *Phys. Rev. D* **48**, 2250 (1993).
- [32] A. Patel and S. R. Sharpe, *Nucl. Phys.* **B395**, 701 (1993).
- [33] M. Golterman, *Nucl. Phys. B, Proc. Suppl.* **73**, 906 (1999).
- [34] M. A. Clark and A. D. Kennedy, *Phys. Rev. D* **75**, 011502 (2007).
- [35] A. Francis, O. Kaczmarek, M. Laine, T. Neuhaus, and H. Ohno, *Phys. Rev. D* **91**, 096002 (2015).
- [36] A. Cheng, A. Hasenfratz, and D. Schaich, *Phys. Rev. D* **85**, 094509 (2012).
- [37] A. Deuzeman, M. P. Lombardo, T. Nunes Da Silva, and E. Pallante, *Phys. Lett. B* **720**, 358 (2013).
- [38] J. B. Kogut, J. Shigemitsu, and D. K. Sinclair, *Phys. Lett.* **145B**, 239 (1984).